

ORIGINAL ARTICLE

Stable knockdown of CREB, HIF-1 and HIF-2 by replication-competent retroviruses abrogates the responses to hypoxia in hepatocellular carcinoma

D Shneur^{1,2}, R Folberg³, J Pe'er², A Honigman^{1,4,5} and S Frenkel^{2,5}

The fast proliferation of tumor cells develops faster than the vasculature, resulting, in most malignant tumors, in generation of hypoxic regions. Hypoxia renders solid tumors resistant to radiation and chemotherapeutics while providing opportunities for tumor-selective therapies targeting tumor hypoxia. Here we exploit two properties of tumors: propagation of tumor cells and ongoing generation of hypoxic regions to construct a system that preferentially leads to the death of tumor cells and thus hinders tumor growth. We constructed murine leukemia virus replication-competent (RCR) viruses that infect only propagating cells. These viruses express small hairpin RNAs (shRNAs) targeting cyclic AMP-response-element binding protein (CREB), hypoxia-inducible factors 1 (HIF)-1 or HIF-2 individually or all three together (X3). These viruses efficiently infected *in vitro* human hepatocellular carcinoma (HepG2 and FLC4) cells and established persistence of the virus and knocked down the expression of the regulators of the hypoxia-responding genes. Knockdown of either HIF-1 or CREB or both in hypoxia reduced the expression of hypoxia-response elements- and CRE-mediated gene expression, diminished cell proliferation and increased caspase-3 activity. We did not detect any significant effect of the efficiently knocked down HIF-2 on any of the functions tested *in vitro*. Moreover, severe combined immunodeficiency mice implanted subcutaneously with HepG2 stably infected with recombinant RCRs showed reduction of tumor growth and vascular endothelial growth factor expression, and no hypoxia-guided neovascularization. Combined treatment (RCRs +doxorubicin) improved efficacy in the context of *in vitro* hypoxia and *in vivo* (with either vACE-CREB or vACE-X3). This synergistic effect may lead to an improved efficacy and safety profile of the treatment that may result in fewer side effects.

Cancer Gene Therapy (2017) 24, 64–74; doi:10.1038/cgt.2016.68; published online 9 December 2016

INTRODUCTION

Hepatocellular carcinoma (HCC) is the third-leading cause of cancer-related deaths globally. Despite improvements in diagnostic and therapeutic approaches, the 5-year survival rate of this cancer is only 7% with a high resistance of HCC to chemotherapy.¹

Hypoxia has an important and complex role in mediating and regulating the progression of the tumor from a microinvasive to metastatic cancer.^{2–4} Unlike normal cells, tumor cells can remain viable in hypoxic environments.⁵ Tumor hypoxia favors the development of metastases resulting in poor survival in patients suffering from various solid tumors.^{2–4}

HCC is a highly angiogenic cancer containing areas of hypoxia. Hypoxia may promote HCC growth, progression and resistance to ionizing radiation and chemotherapeutic drugs.^{4,6} The ongoing development of hypoxic regions in growing tumors provides an opportunity for tumor-selective therapies based on the unique features of hypoxia-induced cell responses.

The adaptive response to hypoxia is orchestrated by a family of transcription factors such as the hypoxia-inducible factors 1 (HIF)-1 and 2 (HIF-2), cyclic AMP-response-element binding protein (CREB).^{7,8}

HIF-1 is a heterodimeric transcription factor that is composed of an O₂-regulated HIF-1 α and constitutively expressed HIF-1 β

subunits. In the presence of O₂, HIF-1 and HIF-2 are subjected to hydroxylation by prolyl-4-hydroxylase domain proteins and are degraded. Under hypoxic conditions, the rate of hydroxylation declines and the non-hydroxylated proteins accumulate.⁹ HIF-1 and HIF-2 bind to hypoxia-response elements (HREs), thereby activating the expression of numerous hypoxia-response genes that are implicated in events such as angiogenesis, cell survival/death, metabolism, migration and metastasis.⁷ Knockdown of HIF-1 in HCC cells by a replication-incompetent adenovector expressing small hairpin RNA (shRNA) targeting HIF-1 abolished cell growth and angiogenesis *in vitro*.¹⁰ Although HIF-1 α and HIF-2 α are highly conserved at the protein level, it was shown that HIF-1 and HIF-2 have distinct, tissue-specific expression patterns.^{11–13}

CREB has crucial roles in cell differentiation, proliferation, cell cycle progression, survival, development and glucose metabolism.^{14,15} Following activation, CREB regulates the expression of genes that suppress apoptosis, induce cell proliferation, regulate metabolism and mediate inflammation and tumor metastasis by binding to the CRE element 5'-TGACGTCA-3'.¹⁵ It was demonstrated in various tumors that CREB promotes tumor progression and resistance to therapy and functions as a survival factor.^{2,16–18} Recently, Park *et al.*¹⁹ demonstrated that CREB

¹Department of Biochemistry and Molecular Biology, IMRIC, The Hebrew University-Hadassah Medical School, Jerusalem, Israel; ²Department of Ophthalmology, Hadassah-Hebrew University Medical Center, Jerusalem, Israel; ³Departments of Pathology, Ophthalmology and Biomedical Sciences, Oakland University William Beaumont School of Medicine, Rochester, MI, USA and ⁴Department of Biotechnology, Hadassah Academic College, Jerusalem, Israel. Correspondence: Dr S Frenkel, Department of Ophthalmology, Hadassah-Hebrew University Medical Center, PO Box 12000, Kiryat Hadassah, Jerusalem 91120, Israel.

E-mail: shahar.frenkel@gmail.com

⁵These two authors contributed equally to this work.

Received 30 May 2016; revised 5 September 2016; accepted 7 September 2016; published online 9 December 2016

blockade by decoy oligonucleotides functionally inhibited trans-activation of CREB, and significantly increased radiosensitivity of multiple human cancer cell lines. We have previously shown that CREB has a pivotal role in the response of HCC to hypoxia cue.² Kovach *et al.*²⁰ also found that total CREB and phosphorylated CREB proteins were both significantly elevated in HCC vs normal liver. Recently it was suggested that the activation of the CREB protein may be associated with tumor progression in HCC, and may serve as a valuable marker of prognosis for patients with this malignancy.²¹

A variety of gene therapy approaches for cancer have failed because it was not possible to achieve effective and specific gene delivery *in vivo* to the tumors.²²⁻²⁶ Selective infection of tumor cells by replication-competent viruses, combined with transfer of antitumoral genes is an attractive strategy for cancer therapy. Such an approach may overcome the limitations revealed in clinical trials with replication-incompetent vector systems that have shown that efficient therapy requires wide or complete dispersion of the antitumoral gene within the tumor tissue.

In the last several years, effective gene delivery was achieved by the use murine leukemia virus (MuLV)-based replication-competent retroviruses (RCR).²⁷ MuLV-derived RCRs have a strict requirement for cell division, because of an absence of a nuclear localization signal for active transport across intact nuclear membranes in quiescent cells; infection is innately restricted to propagating cells.^{28,29} As most normal cells in the body are quiescent, RCRs-mediated gene transfer *in vivo* is largely restricted to the rapidly growing cells of malignant tumors. These viruses infect cells without a known cytopathic effect, spread through tissues, and stably integrate their genome into that of the host cell offering a unique potential for persistence of the virus and a permanent antitumoral effect.²⁹⁻³¹ It was demonstrated that RCRs are capable of achieving highly efficient replicative spread and gene delivery throughout solid tumors *in vivo* and are carried to developing metastases.^{32,33}

Viral delivery of shRNA presents an efficient system for *in vivo* delivery of RNAi therapeutics that enables the RNAi therapeutic to traverse biological barriers *in vivo*.³⁴ In this work we combine the efficient and selective infectivity of propagating cells by the MuLV with the specific knockdown function of shRNA to target individually or simultaneously the three regulators of hypoxia-responding genes: HIF-1, HIF-2 and CREB. Expression of a versatile multiple shRNA cassettes targeting several genes involved in the response to one stress is an efficient way to abrogate cellular responses.^{35,36} Because MuLV-infected cells cannot be re-infected by MuLV, the expression of the three shRNAs from one virus should overcome this limitation and lead to the expression of the three shRNAs in each infected cell.

Doxorubicin (DOX) is a chemotherapeutic agent of the topoisomerase inhibitor family that is widely used for the treatment of cancers. Its use is associated with severe known side effects including congestive heart failure, which may lead to severe cardiomyopathy and death. Moreover, it was shown that combining inhibition of CREB phosphorylation with DOX treatment was significantly more effective in HepG2 (ref. 37) and mesotheliomas.³⁸ It was demonstrated that DOX impairs the cellular hypoxia responses via impairment of the transcriptional response of HIF-1.³⁹ In this study, we demonstrate that knock-down of CREB and HIF-1 in combination with treatment with DOX improves the killing of HepG2 cells in hypoxia. This finding may lead to a reduction in the DOX-effective clinical dose and thus diminish the harmful side effects induced by DOX treatment.^{39,40}

MATERIALS AND METHODS

Cell culture

Human HCC HepG2 and FLC4 cell lines (verified by STR analysis) were grown in Dulbecco's modified Eagle's medium (DMEM) supplemented with

10% fetal bovine serum, 2 mM glutamine, 100 IU ml⁻¹ penicillin, 100 µg ml⁻¹ streptomycin (Biological Industries, Beit Haemek, Israel) and incubated at 37 °C in a humidified atmosphere with 5% CO₂. To culture cells in hypoxia, the cells were incubated in hypoxia jars at 0.5% O₂ (AnaeroGen Oxoid, ThermoFisher Scientific, Waltham, MA, USA).

Plasmids and viruses

The plasmid pACE-GFP (a kind gift from Professor Noriyuki Kasahara, Los Angeles, California) contains a full-length replication-competent amphotropic MuLV provirus with an additional internal ribosome entry site (IRES)-GFP cassette flanked with *Bsi*WI and *Not*I restriction enzymes sites. This cassette was replaced by oligonucleotides harboring the H1 promoter driving the transcription of one of the following shRNA sequences:

5'-GAGAGAGGTCCTAATGTTCAAGAGACATTAGACGGACCTCTCTCTTTT-3' (pACE-CREB). 5'-CTAACTGGACACAGTGTGTTTAAATATATGAAAACACACTGTGTCAGTTAGTTTTT-3' (pACE-HIF-1). 5'-ATTAAGTATTCTGATCCGATTA TAAAGGATCAGAATACTTTAATAAGTTTTT-3' (pACE-HIF-2). 5'-CTAACTGGA CACAGTGTGTTAATATATGAAAACACACTGTGTCAGTTAGTAAAGTCGACTCG CTTATTAAGATTCTGATCCGATTATAAAGGATCAGAATACTTTAATAAGAATG GCGCGTCTTCGAGAGAGGTCCTGCTAATGCCTGAACCATTAGACGGACCTC TCTTTTTT -3' (pACE-X3). This vector includes shRNA targeting CREB, HIF-1 and HIF-2. 5'-ACCAAGATGAAGAGACCAACCTGAACCATTGGTGCTCT CATCTGGTTTTT-3' (pACE-NT. Non-target shRNA). See Figure 1 for a schematic presentation of the vectors.

Virus production

HEK293T cells were transiently transfected with either one of the plasmids, described above and in Figure 1, using FuGENE HD (Promega Corp., Madison, WI, USA). The medium was harvested 48 h later, filtered (MILLEX-HV, PVDF 0.45 µm) and stored at -80 °C.

Western blot analysis

Equal amounts of total protein were prepared in Laemmli sodium dodecyl sulfate loading buffer, resolved on 10% sodium dodecyl sulfate-polyacrylamide gel electrophoresis and transferred to PVDF membranes (Millipore, Billerica, MA, USA). For detection of CREB, HIF-1 or HIF-2, membranes were blocked for half an hour in TBS-T (20 mM Tris pH 7.4, 150 mM NaCl, 0.1% Tween-20) containing 5% skim milk (Difco, Franklin Lake, NJ, USA) and incubated overnight (4 °C) with either CREB (Santa Cruz, Dallas, TX, USA), HIF-1 (Abcam, Cambridge, MA, USA), HIF-2 (Novus Biologicals, Littleton, CO, USA) or α-tubulin (Santa Cruz) primary antibodies. The blots were washed, incubated with a secondary horseradish peroxidase (HRP)-conjugated antibody (Promega Corp.) for 1 h, then washed again and were visualized using the enhanced chemiluminescence system (Promega Corp.). Blots were scanned by the MiniBIS Pro (DNR, Jerusalem, Israel), and band intensities were quantified by the TINA 20 program (Raytest, Straubenhardt, Germany).

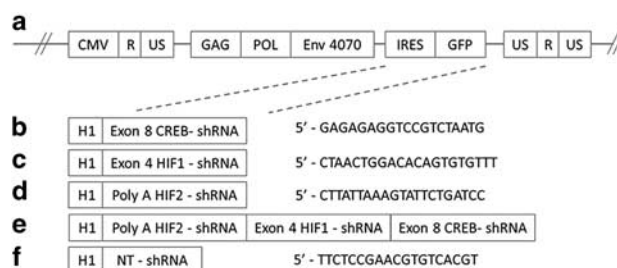


Figure 1. A schematic presentation of the various replication-competent viruses (RCRs). (a) A proviral construct of pACE-GFP. (b-f) The IRES-GFP sequences were replaced with an H1 promoter driving the transcription of the various small hairpin RNAs (shRNA) targeting cyclic AMP-response-element binding protein (CREB) (b), hypoxia-inducible factor (HIF)-1 (c), HIF-2 (d), all three genes (e) and a non-target sequence (f). The DNA sequence of the various shRNAs is marked.

Quantitative real-time PCR

RNA was extracted from the cells using the SV Total RNA isolation System (Promega Corp.), according to the manufacturer's instructions. The purified RNA samples were subjected to reverse transcription using GoScript (Promega Corp.), monitored by quantitative 7900HT real-time PCR apparatus (Applied Biosystems by Life Technologies Corp., Carlsbad, CA, USA) utilizing the GoTaq Real-Time PCR reagents (Promega Corp.) and the specific primers: CREB: fp- 5'-CCCAGCACTTCTACACAGCCTGC-3', rp5'-CG AGCTGCTCCUGTTCTT CATTAGACG-3', HIF-1: fp5'-GGGATTAACCTCAGT TGAACCTAACTGG-3', rp5'-CCTTTTTACAAGGCCATTTCTGTGTG-3', HIF-2: fp5'-ACAAGGTGTCAG GCATGGCAAGC-3', rp5'-CGTTCACCTCACAGTCA TATCTGG-3'. The results were normalized to the cellular house-keeping gene GAPDH: fp5'-CCATCTCCAGGA GCGAGATCC-3', rp5'-GCAATGA GCCCCAGCTTCTCC-3'.

Luciferase assay

HepG2 cells were infected with vACE-HIF-1, vACE-HIF-2, vACE-CREB, vACE-X3 or vACE-NT and seeded in 6-well plates at a concentration of 500 000 cells per well for 24 h. The infected cells were co-transfected (3 µg DNA) with either the CRE-mediated luciferase (*luc*) reporter plasmid vector, pCRELuc² or by the HRE-controlled *luc* gene reporter plasmid⁴¹ together with 0.25 µg of an expression vector expressing the Renilla luciferase gene, pHRLSV40, as a transfection control (Promega Corp.) using FuGENE HD (Promega Corp.). Each experimental procedure was performed with five biological repeats and three technical repeats. Luciferase activity was determined in triplicates 48 h post transfection, according to the manufacturer's instructions (Dual Luciferase reporter assay system, Promega Corp.) by an automatic Mithras LB 940 photoluminometer (Berthold Technologies, Oak Ridge, TN, USA). The results were normalized to Renilla luciferase activity.

VEGF expression assay

Infected HepG2 cells with either one of the viruses mentioned above were seeded at a concentration of 3000 cells per well in 96-well plates and incubated at normoxic and hypoxic conditions for 24 h (five biological repeats). The supernatant vascular endothelial growth factor (VEGF) levels were quantified by enzyme-linked immunosorbent assays following the manufacturers' instructions (R&D Systems, Minneapolis, MN, USA) in three technical repeats. VEGF levels were normalized to the cell count and to the VEGF levels from cells infected with vACE-NT.

Cell viability and activation of caspase-3

Infected cells with one of the recombinant viruses mentioned above were seeded at a concentration of 3000 cells per well in 96-well plates (six biological repeats) and incubated at normoxic and hypoxic conditions up to 72 h. At the indicated time points, cell's viability and caspase-3 activity was determined by the Fluorescent Cell Viability and Caspase-Glo 3/7 Assays (Promega Corp.) according to the manufacturer's instructions with three technical repeats.

Xenograft mouse model

The animal protocol used in this study was approved by the IACUC of the Hebrew University of Jerusalem. HepG2 and FLC4 cells infected with either one of the recombinant viruses were harvested and 4×10^6 cells in 100 µl were injected subcutaneously (SC) above the foreleg of severe combined immunodeficiency (SCID) mice (C.B-17/ICRHSD-PRKDC-SCID) weighing 20–24g (about 3 weeks of age), five mice in each group to allow descriptive statistics. Animals (males and females) were randomly assigned to each treatment group, keeping an even distribution of sexes between groups. DOX (20–75 mg kg⁻¹) was administered intraperitoneal (IP) twice weekly starting at 14 days post inoculation of the cells. Tumor growth was monitored following IP injection of D-luciferin 300 mg 0.1cc⁻¹ per mouse (Promega Corp.) 10 min before imaging. Mice were anesthetized with isoflurane and bioluminescence was measured with the IVIS *InVivo* System (Caliper Life Sciences, Waltham, MA, USA). No animals were excluded from the analysis, and there was no blinding during the experiments.

Immunohistochemistry

Prior to euthanasia, mice were injected IP with Hypoxyprobe (Hypoxyprobe, Burlington, MA, USA) according to the manufacturer's instructions. After excision, tumors were photographed, measured and fixed in 4%

formaldehyde for routine processing and embedding. Four-micron thick sections were cut and stained with hematoxylin–eosin. For light microscopic immunohistochemistry, paraffin sections were cut at 4 µm. Slides were deparaffinized using xylene and absolute ethanol, rinsed in distilled water, exposed to H₂O₂ for 5 min or antigen unmasking. The antigen unmasking solution (citrate buffer, Thermo Scientific, Fremont, CA, USA) was heated in a steamer to 105 °C for 10 min, then cooled to room temperature. The sections were rinsed with PBS IHC for 2 min (CELL Marque, Rocklin, CA, USA) and blocked with CAS-Block for 5 min (Invitrogen, Paisley, UK). Slides were rinsed with PBS IHC and reacted with primary antibodies targeting CD34 (Abcam), and FITC-MAb1 (Hypoxyprobe) followed by a rinse in PBS IHC and reaction with secondary antibodies: MACH-2 rabbit HRP-Polymer (Biocare Medical, Concord, CA, USA) and HRP linked to rabbit anti-FITC, accordingly. Sections were rinsed with PBS IHC and incubated with AEC (CELL Marque) for 10 min. Sections were rinsed in distilled water and PBS IHC and counterstained with Mayer's hematoxylin, and coverslipped with a permanent mounting medium (AquaSlip, American MasterTech, Lodi, CA, USA).

Slides were photographed with a Nikon ECLIPSE Ti microscope. A grid of 19 × 14 square regions of interest (ROIs) measuring 405 × 405 µm each covering the entire scanned image. A mask of the secondary antibody pixels was created using ImagePro 9 (Media Cybernetics, Rockville, MD, USA), and the number of pixels per ROI was counted. Pixel count from matching ROIs was correlated between endothelial cells and hypoxia over the entire section for each slide. ROIs with a hypoxia pixel count over the background level were labeled 'hypoxic', and the rest were labeled 'normoxic'.

Statistical analysis

In vitro experiments with at least three biological and three technical repeats for each data point yield sufficient statistical power. For animal experiments we chose five animals per group to allow descriptive statistics on the one hand while minimizing the use of animals to accommodate the ethical restrictions on the other hand.

Statistical analysis was performed with JMP 12.0 (SAS, Cary, NC, USA). Analysis of variance was used to compare messenger RNA (mRNA) levels, luciferase activity in relative light units and the relative VEGF enzyme linked immunosorbent assays (ELISA) expression levels. Multivariate analysis of variance for repeated measures was used to compare the cell viability, caspase-3 activity (Figure 3) and the growth rates of the tumors within the mice (Figure 4). Analysis of variance and Dunn's Multiple Comparison (vACE-NT served as control) were used to compare viability and caspase-3 activity levels at the last time point (Figure 3 and Supplementary Figures 1 and 2). A pairwise two-tailed correlation between CD34 and HypoxyProbe pixel counts was performed and the correlation coefficient was compared between hypoxic and normoxic ROIs (Figure 5). The variance was similar between the compared groups.

RESULTS

Construction and functional analyses of MuLV replication-competent viruses expressing shRNA targeting hypoxia-responsive transcription factors

Two of the features that characterize tumors are tumor cells replication and ongoing development of hypoxic regions. These two characteristics served us in constructing vectors that will infect only dividing cells and harm only hypoxic cells. To achieve this goal, we constructed MuLV-based RCRs expressing shRNAs targeting the major regulators of the cellular responses to hypoxia. More specifically, we replaced the GFP coding region in the plasmid vector pACE-GFP³³ with an H1 promoter and sequences of shRNAs targeting either CREB, HIF-1 or HIF-2 (pACE-CREB, pACE-HIF-1 and pACE-HIF-2, respectively) or transcribing a non-target sequence (pACE-NT) as a control. Because MuLV-infected cells cannot be re-infected by MuLV, and we aim to knockdown all three regulators in each cell, we cloned a sequence harboring a polycistronic RNA molecule coding for shRNA targeting all three genes (pACE-X3) (Figure 1).

To determine if infection with the recombinant RCRs will generate a knockdown infection, we produced viral particles by transfection of HEK293T cells with the recombinant plasmid

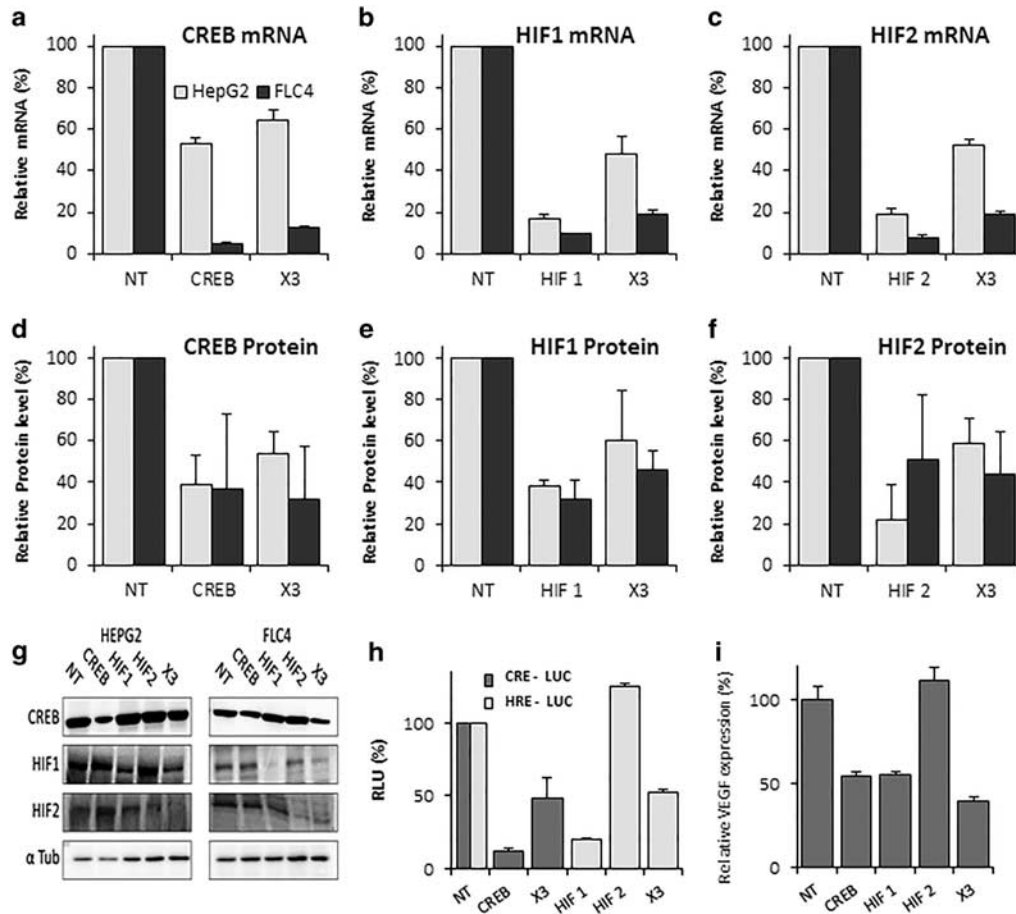


Figure 2. Quantification of the efficiency of the knockdown in infected cell lines and the effect on the expression of regulated genes. Cells, HepG2 and FLC4 were infected with each of the recombinant replication-competent retroviruses (RCRs) as specified in the figure and cultured in hypoxic conditions for 24 h. Purified mRNA was quantified by real-time quantitative PCR. Levels of messenger RNA (mRNA) were normalized to mRNAs in cells infected with vACE-NT (set as 100%) (a–c). Proteins were quantified following western blot analysis (g), and band intensities were compared with those of α -tubulin and to band intensity of cells infected with vACE-NT (set as 100%) (d–f). Levels of all measured mRNAs (a–c) and proteins (d–f) were statistically significantly lower when compared with vACE-NT-infected cells in both cell lines ($P < 0.05$). HepG2 cells infected with the various RCRs were transiently transfected with either pCRE-LUC or pHRE-LUC. Luciferase activity was determined after 48 h of exposure to hypoxia relative to cells infected with vACE-NT (presented as 100%) for each transfection. CRE (dark columns) and hypoxia-response elements (HRE) (light columns) mediated LUC activity are presented in relative light units ($P < 0.001$) (h). The levels of vascular endothelial growth factor (VEGF) secreted by HepG2 cells were determined by enzyme-linked immunosorbent assays as described in the Materials and methods section. The VEGF secretion levels in hypoxia relative to normoxia were normalized to the ratio in vACE-NT-infected cells ($P < 0.01$) (i). α -Tub = α -tubulin. Bars represent mean \pm s.d. for each measurement.

vectors (see above) and the virus particles were collected with the growth media 48 h post transfection. On the basis of monitoring GFP-producing cells following infection by vACE-GFP (results not shown), both the HepG2 and the FLC4 cells were infected for about 2 weeks to reach a fully infected culture. The efficiency of knockdown of HIF-1, HIF-2 or CREB was determined by RT-qPCR and western blot analyses. The assays were carried out following incubation of the cells for 24 h in hypoxic conditions to determine the knockdown of HIF-1 and HIF-2. As infection with non-target shRNA (vACE-NT) did not change significantly, the expression of any of the three tested genes relative to non-infected cells and knockdown efficiencies by the other viruses was compared with those in cells infected with vACE-NT and with a control gene, *GAPDH*.

The levels of CREB mRNA in HepG2 and FLC4 cells infected with vACE-CREB were reduced by 65% and 95% and the CREB protein by 61% and 63%, respectively. The knockdown of HIF-1 and HIF-2 in cells infected with either vACE-HIF-1 or vACE-HIF-2 was very

efficient in HepG2 cells: 81–83% reduction of the mRNA and 62 and 78% of the HIF-1 and HIF-2 proteins. A similar reduction was found in FLC4 cells: 90% and 92% of mRNA and 68% and 49% of HIF-1 and HIF-2 proteins, respectively. Although less efficient than in cells infected with RCR targeting each gene individually, infection with the RCR expressing the multi-shRNA, vACE-X3 resulted in a reduction of CREB mRNA by 47% and 95% and the CREB protein by 66% and 68%, for HepG2 and FLC4, respectively. The reduction of HIF-1 and of HIF-2 mRNAs and proteins in vACE-X3-infected HepG2 cells was 52% and 48% in the mRNA of both genes and 40% and 41% in the protein level, respectively. In FLC4 vACE-X3-infected cells, the reduction of HIF-1 mRNA and protein level was 81% and 54%, respectively. The reduction of HIF-2 mRNA and protein level was 81% and 56%, respectively. (Figure 2). The effective downregulation of the mRNAs does not always correlate to a similar reduction in the protein levels probably due to differences in the stability of the proteins in the two cell lines.

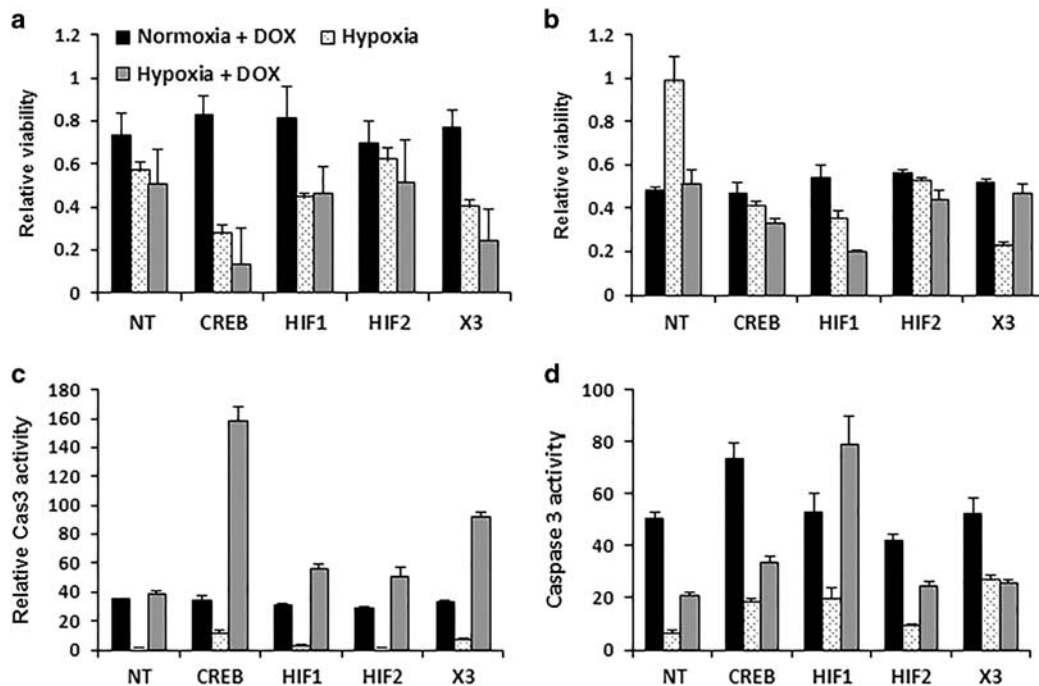


Figure 3. The role of cyclic AMP-response-element binding protein (CREB), hypoxia-inducible factor (HIF)-1 and HIF-2 in protecting HepG2 and FLC4 cells from hypoxia-induced apoptosis and on the response to treatment with doxorubicin (DOX). HepG2 (a, c) and FLC4 (b, d) infected with each of the viruses specified in the figure were cultured for 72 h. Viability (a, b) and activation of caspase-3 (Cas3) (c, d) were determined every 24 h. The relative viability and activation of caspase-3 after 72 h of hypoxia (light gray columns), and those after treatment with 1 mM of DOX in normoxia (black columns) and hypoxia (dark gray columns) were normalized to cells infected with each respective replication competent retroviruses in normoxia ($P < 0.01$ for all comparisons). Bars represent mean+s.d. for each measurement.

The effect of the knockdown of HIF-1, HIF-2 and CREB on the expression of CRE- and HRE-mediated gene expression

To monitor the effect of the virus-mediated knockdown of CREB, HIF-1 and HIF-2 on activation of downstream genes in the stably infected HepG2 cells with one of the four RCR viruses (vACE-CREB, vACE-HIF-1, vACE-HIF-2 or vACE-X3), cells were transfected with either plasmid pCREluc, CRE-mediated luciferase gene expression or pHREluc in which *luc* gene expression is activated by either HIF-1 or HIF-2. Luciferase activity was determined in normoxia and hypoxia 48 h post transfection. As expected, reduction of 61% in CREB or 62% in HIF-1 proteins (Figures 2d and e) resulted in reduction of 88% and 80% in CRE or HRE-mediated *luc* activity, respectively (Figure 2h). In cells infected with vACE-X3, CRE- or HRE-mediated *Luc* activity was reduced by more than 50% (Figure 2h). This result correlates with the less efficient knockdown of CREB and HIF-1 by vACE-X3 relative to the viruses expressing either one of the shRNA individually (Figures 2d and e). Knocking down HIF-2 did not reduce the expression of HRE-mediated *luc* relative to cells infected with vACE-NT. Because HIF-1 and HIF-2 recognize the same activation domain, HRE, the HRE-mediated *luc* expression in cells infected with vACE-HIF-2 might have been activated by the more efficient HIF-1.

The role of HIF-1, HIF-2 and CREB in the secretion of endogenous VEGF in hypoxia

In response to hypoxia, solid tumors stimulate tumor angiogenesis through HIF-induced expression of proangiogenic factors. One of the HIF-1- and CREB-activated proangiogenic growth factors is the VEGF.⁴²⁻⁴⁵

To monitor the effect of the functionality of the CREB, HIF-1 and 2 on VEGF in stably infected HepG2 cells with one of the four RCR viruses (vACE-CREB, vACE-HIF-1, vACE-HIF-2 or vACE-X3), the cells were cultured in normoxic and hypoxic conditions for 24 h (Figure 2i).

Targeting either CREB or HIF-1 (vACE-CREB and vACE-HIF-1) diminished VEGF expression in HepG2 cells by 45% each (Figure 2i) at hypoxia vs normoxia. However, targeting HIF-2 had only a minor impact on VEGF expression in these cells. Targeting all three genes with the vACE-X3 showed a combined effect reducing the expression of VEGF by 58%. This result is consistent with the finding that both CREB and HIF-1 regulate VEGF expression in hypoxia.

The role of CREB, HIF-1 and HIF-2 in protecting HepG2 and FLC4 cells from hypoxia-induced apoptosis

We next analysed the contribution of each of the three transcription factors to the survival of HepG2 and FLC4 in hypoxia. Cells stably infected with MuLV expressing shRNAs targeting CREB, HIF-1, HIF-2 or with the virus expressing the polycistronic shRNA cassette (X3) were incubated up to 72 h under either normoxic or hypoxic conditions. At different time points during cells growth, cell viability, relative to time zero and caspase-3 activation relative to living cells at each time point and to time zero were determined (Supplementary Figures 1 and 2). At 72 h of hypoxia, only about 27% of HepG2 and 41% FLC4 cells infected with vACE-CREB survived the hypoxia cue, whereas 56% of HepG2 and 98% of FLC4 cells infected with vACE-NT was observed (Figures 3a and b). This indicates that FLC4 cells tolerate hypoxia better than HepG2 cells. Knockdown of HIF-1 had a smaller effect than knockdown of CREB on the survival of HepG2 cells in hypoxia (44% vs 27% survived). In FLC4 after 72 h of hypoxia the knockdown of either CREB or HIF-1 had a similar effect on their survival (35% vs 41%) (Figure 3b). Exposure of HepG2 cells infected with vACE-HIF-2 to 72 h of hypoxia had no significant effect on survival of these cells relative to cells infected with vACE-NT (Figure 3). While vACE-HIF-2-infected FLC4 cells showed a 48% reduction in cell viability in hypoxia. It is therefore not surprising

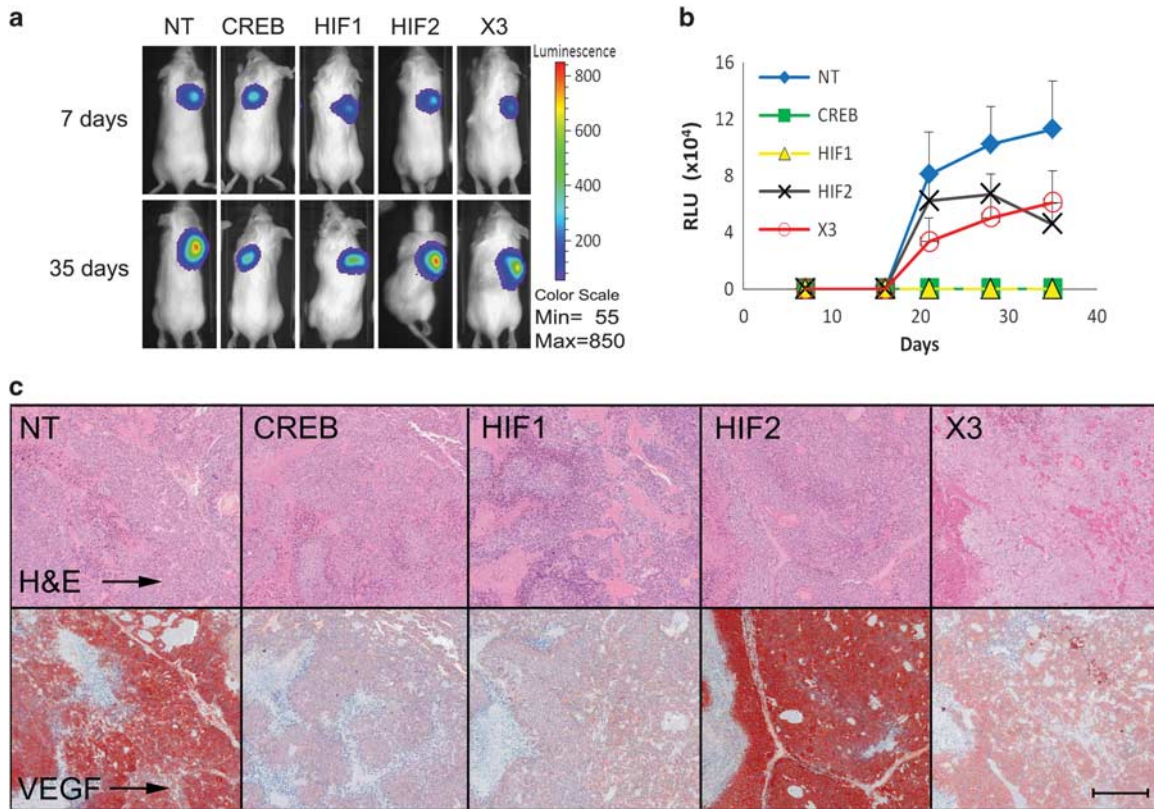


Figure 4. Testing the effect of cyclic AMP-response-element binding protein (CREB), HIF-1 and 2 on tumor growth *in vivo* in a mouse xenograft model. Severe combined immunodeficiency mice were implanted with 4×10^6 HepG2 cells as described in Materials and methods section. Tumor growth was monitored every 7 days with the IVIS *In Vivo* System. Images of light emission from representative mice taken on days 7 and 35 are presented. The same color scale was used for all mice at both time points (a). Relative light units (RLU) measurements were normalized to the readings on day 7 post injection and plotted along the extent of the experiment. Each point represents the mean+s.e. (b). At the end of the experiment, tumors were harvested for histopathological analysis. Hematoxylin-eosin staining and the corresponding vascular endothelial growth factor immunohistochemistry of tumors are presented in (c). ($\times 4$ magnification, scale bar 100 μm).

that knockdown of all three transcription factors by vACE-X3 diminished survival of FLC4 cell (23% remained) more than its effect on HepG2 cells (40%) ($P < 0.01$ for all comparisons). The increase in cell mortality ($\times 2$) of cells with diminished CREB relative to cells infected with vACE-NT correlates with the increase in activated caspase-3 in HepG2 ($\times 11$) and in FLC4 ($\times 3$) cells, relative to time zero. Knockdown of HIF-1 had a lesser but still significant effect on the activation of caspase-3 in the cells (Figure 3, Supplementary Figures 1 and 2). Knockdown of HIF-2 did not affect the activation of caspase-3 in both cell lines. Infection with vACE-X3 that barely affected the activation of caspase-3 in HepG2, had a marked effect in FLC4 cells ($P < 0.001$), in correlation with cell death (see above; Figure 3, Supplementary Figures 1 and 2).

The results presented here indicate that CREB, more than HIF-1 and HIF-2, has a pivotal role in the survival of HepG2 in hypoxic conditions *in vitro*, whereas in FLC4 CREB and HIF-1 have a similar role.

The effect of combined treatment by RCR-mediated knockdown of hypoxia-responding control elements and drug treatment on cell survival

DOX-induced tumor cell death was linked with both CREB and HIF-1 pathways.^{37,39} We hypothesized that combining the knockdown of the hypoxia-responding factors with DOX treatment would have a synergistic effect and may reduce the effective

clinical dose of DOX and thus diminish the side effects of the drug. To test this hypothesis, we measured survival of RCR-infected HCC cells treated with varying concentrations of DOX and determined the minimal lethal dose of DOX on HepG2 and FLC4 tumor cells. The cells were treated with increasing concentrations of DOX and cultivated in normoxic or hypoxic conditions. On the basis of these experiments (not shown), HepG2 and FLC4 cells expressing the various shRNAs were treated with $1 \mu\text{M}$ DOX, the minimal concentration that diminished the growth of the treated cells in normoxia. Cell viability and caspase-3 activation following treatment with DOX were similar in cells infected with the various RCRs in normoxia (Figure 3, black columns, Supplementary Figures 1b and 2b).

In normoxic conditions, 72 h after administering DOX, cell viability decreased by 27% and 52% in HepG2 and FLC4 cells infected with vACE-NT, respectively. At the same time caspase-3 activation in HepG2 and in FLC4 increased by 35- and 24-fold, respectively (Figure 3, black columns). At normoxia knockdown of CREB, HIF-1 and HIF-2 did not contribute to cell death or caspase-3 activation induced by DOX.

As described above at 72 h of hypoxia, knockdown of CREB reduced the viability of the two HCC cell lines reaching mortality of 73% of HepG2 and 48% of FLC4, relative to time zero (Figure 3). Combining hypoxia and treatment with DOX of these infected cells resulted in a decrease of 87% in the viability of HepG2 and of 65% of FLC4-infected cells (Figure 3 and Supplementary Figures 1c and 2c). The increase of caspase-3 activity correlated with the

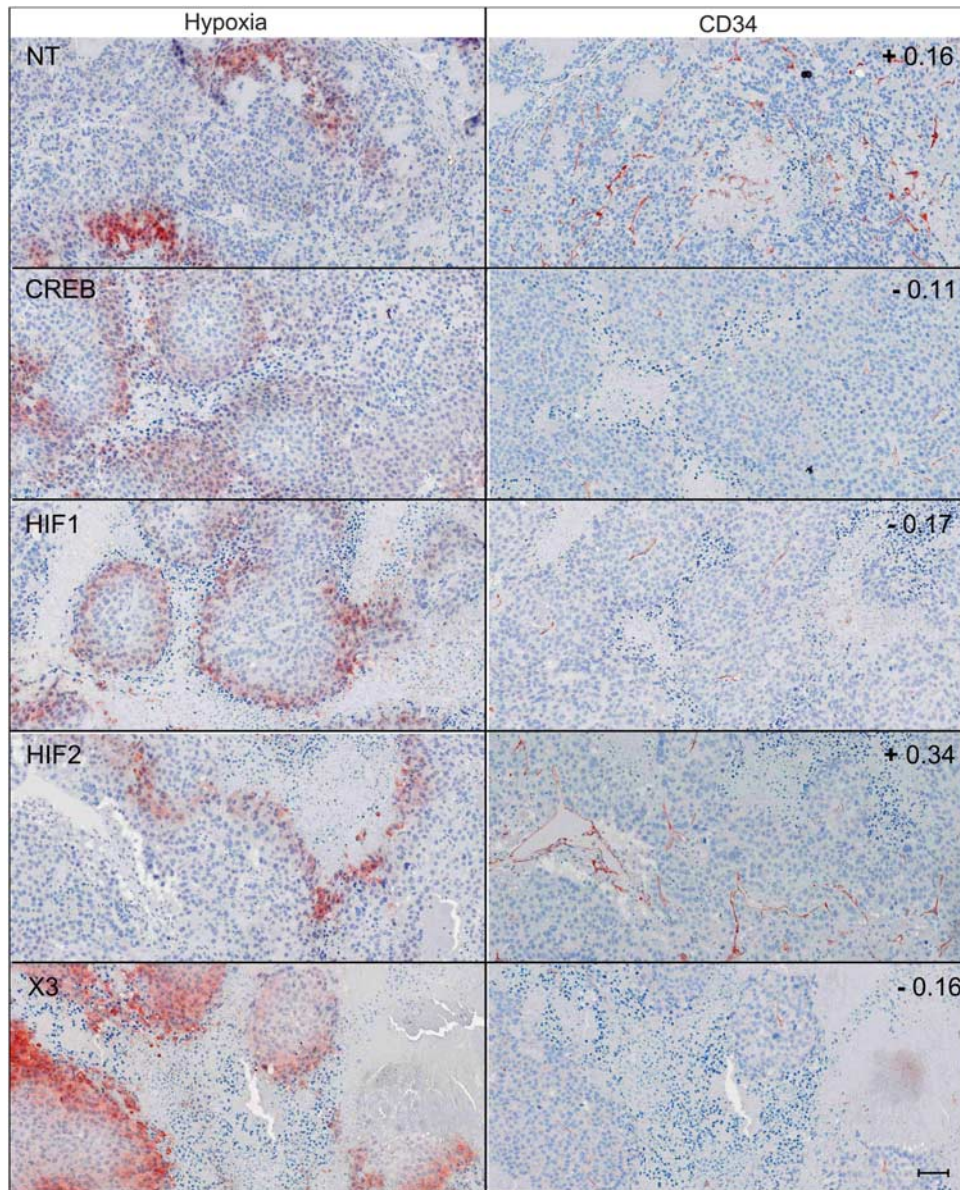


Figure 5. Immunohistochemical analysis of hypoxia and blood vessels (CD34) of the tumors. Tumors infected with replication-competent retroviruses expressing small hairpin RNA (shRNA)-targeting genes specified on the left column were stained for hypoxia (left column) and for blood vessels (right column) as described in the Materials and methods section. It is clear that knockdown of CREB, HIF-1 and all three genes together (X3) abolished neovascularization within the tumors. In tumors infected with the non-target shRNA or with shRNA targeting HIF-2 blood vessel growth toward the hypoxic regions is noticed. Correlation between the amount of CD34 and hypoxia staining is presented in the top right column for each virus. ($\times 10$ magnification, scale bar 500 μm).

mortality of the treated cells. FLC4 cells showed a milder response than HepG2 to the combined treatment of CREB knockdown and DOX in hypoxic conditions. The effect of DOX treatment of HepG2 cells and FLC4 infected with vACE-CREB in hypoxia was 5 and 1.6 times, respectively, relative to vACE-NT-infected treated cells. In both cell lines we see an additive effect to the combination of hypoxia and CREB knockdown.

Knockdown of HIF-1 had no additive effect in combination with DOX in normoxia in both cell lines (Figure 3). In hypoxia, FLC4 cells were more sensitive than HepG2 to the combined treatment of knockdown of HIF-1 and DOX. In hypoxia, only 21% of the vACE-HIF-1 FLC4-infected cells survived the combined treatment (vs 74% of vACE-NT infected cells), whereas 46% of the HepG2-infected cells survived DOX treatment similar to HepG2 cells infected with vACE-

NT (50%). The changes in caspase-3 correlated the changes in survival under these conditions. Similar to the different sensitivity of the two cell lines to HIF-2 knockdown in hypoxia, combination of DOX and vACE-HIF-2 infection had no additive effect on HepG2 cells, but had an effect on FLC4 cells (43% survival vs 74% survival of vACE-NT-infected cells), without a matching significant effect on the activation of caspase-3 (Figure 3).

Treatment with DOX of either HepG2 or FLC4 cells infected with vACE-X3, expressing all three shRNAs, resulted in a similar, although a milder effect on survival and caspase-3 activity in hypoxia relative to the knockdown of only CREB (Figure 2). These results may be due to a lower activity of the shRNAs in vACE-X3 relative to viruses expressing each shRNA individually (Figure 2).

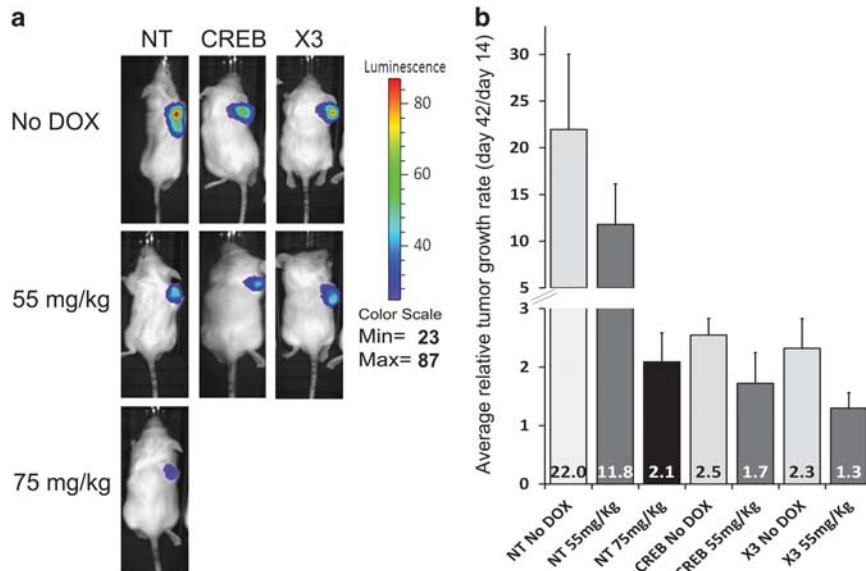


Figure 6. Effect of combined treatment on tumor growth monitored by light emission. HepG2 cells stably expressing the *luc* gene and infected with the viruses specified above were implanted subcutaneous in severe combined immunodeficiency (SCID) mice. After 3 weeks, the mice were injected twice a week with doxorubicin (DOX) in the concentrations specified in the picture. Tumor growth was monitored by light emission as described in Figure 4. **(a)** One mouse from each group at day 42 is depicted. A scale bar of light emission is localized on the right side of the picture. **(b)** The average (+s.d.) relative tumor growth rate between days 14 and 42 is presented on each bar.

Put together, HCC cells infected with the RCR vectors expressing the various shRNAs increase the sensitivity of cells to DOX treatment.

Effect of knockdown of CREB HIF-1 and HIF-2 on tumor growth
SCID mice were inoculated SC with HepG2 cells stably infected with either vACE-NT, vACE-CREB, vACE-HIF-1, vACE-HIF-2 or vACE-X3. The rate of growth of the tumors was monitored by a CCD camera. The results presented in Figure 4 clearly demonstrate that knockdown of either CREB or HIF-1 abrogates the tumor growth. In correlation with the *in vitro* results (Figure 3a), tumor growth of cells infected with vACE-X3 was affected less than tumors infected with either vACE-CREB or vACE-HIF-1 (Figures 4a and b). Although no effect on tumor cell survival was noticed *in vitro* following knockdown of HIF-2, *in vivo* knockdown of HIF-2 did affect the growth rate of the HepG2 tumors in mice moderately (Figure 4b).

Effect of knockdown of CREB, HIF-1 or HIF-2 on VEGF and blood vessels distribution in HCC-growing tumors
For histopathological analyses tumors were excised from the mice after 35 days. The hypoxic regions were detected by Hypoxyprobe technology and VEGF and blood vessels were detected by antibodies targeting VEGF or CD34. In correlation with the *in vitro* result presented Figure 5i, the expression of VEGF in tumors harboring vACE-CREB, vACE-HIF-1 or vACE-X3 was reduced dramatically (Figure 4c). This result, in agreement with the finding that both CREB and HIF-1 are essential for activation of VEGF expression,⁶ demonstrates that infection of HCC tumor cells with the vACE-CREB, vACE-HIF-1 and vACE-X3 may serve to abolish hypoxia-mediated neovascularization in growing tumors. Similar to the *in vitro* experiments, knockdown of HIF-2 had no effect on VEGF expression in the growing HCC xenografts.

The reduction in VEGF expression by targeting CREB and/or HIF-1 is expected to diminish blood vessels growth toward the hypoxic regions. Indeed, CD34 stained blood vessels (Figure 5

right panels marked red) directed toward the hypoxic regions (Figure 5 left panels marked red) in tumors infected with vACE-NT or with vACE-HIF-2. However, only scant vessels were noticed in tumors infected with vACE-CREB, vACE-HIF-1 or vACE-X3. This was highlighted by correlating the amount of blood vessel staining to the level of hypoxia in these tumors (marked on the upper right corner of the right column) with a positive correlation between CD34 and hypoxia in tumors infected with vACE-NT or vACE-HIF-2 (0.16 or 0.34, respectively), and a negative correlation in tumors infected with vACE-CREB, vACE-HIF-1 or vACE-X3 (−0.11, −0.17 or −0.16, respectively).

Effect of combined treatment on tumor growth

SCID mice were inoculated SC with HepG2 cells stably infected with either vACE-NT, vACE-CREB or vACE-X3. Tumors were allowed to grow for 2 weeks, and then mice were injected IP with DOX (20–75 mg kg^{−1}) twice a week (data not shown). A concentration of 75 mg kg^{−1} was sufficient to almost completely eradicate the tumors even in vACE-NT-infected tumors (Figure 6). To assess the combined effect we used a sub-lethal dose (55 mg kg^{−1}). At 6 weeks, similar to the *in vitro* findings above, tumors infected with either vACE-CREB or vACE-X3 were slower to grow. The addition of DOX reduced the growth rate of all tumors. Tumor growth measured by light emission was compared between day 42 and day 14 post inoculation. Tumors infected with vACE-NT grew 22-fold in this time period, whereas vACE-CREB- and vACE-X3-infected tumors grew by only little over two-folds. The growth rate of DOX-treated tumors infected with vACE-NT was reduced by 45%. The combined treatment of infection with either vACE-CREB or vACE-X3 resulted in about 90% reduction in tumor growth (Figure 6).

DISCUSSION

In this work we exploited two properties of tumors—propagation of tumor cells and generation of hypoxic regions within the

growing tumors—to construct a system that will preferentially lead to the death of tumor cells and thus hinder tumor growth.

Tumor hypoxia is considered to be a potential therapeutic problem because it renders solid tumors more resistant to ionizing radiation and chemotherapeutic drugs.⁴⁶ However, the ongoing development of hypoxic regions in growing tumors provides an opportunity for tumor-selective therapies. The RCRs developed in this work infect preferentially tumor cells and knockdown the ability of tumor cell to withstand hypoxia. Moreover, the stably infected cells produce infectious RCRs that spread within the replicating cells within the tumor and thus generate an infectious knockdown of the genes controlling the hypoxia responses within the tumor. It was demonstrated that MuLV-based RCRs infect efficiently different tumors such as colorectal cancer, gliomas and others.^{30,47–51}

Infection with the RCRs described in this work established stable proviruses expressing the shRNAs that specifically and efficiently knocked down the target genes: CREB, HIF-1 or HIF-2. Under hypoxic conditions *in vitro* knockdown of CREB and/or HIF-1 gene expression by the recombinant RCRs resulted in reduced tumor cell survival, increased activation of caspase-3 and in a reduction in VEGF secretion (Figures 2 and 3). In mice, knockdown of CREB and HIF-1 resulted in attenuation of tumor growth, of VEGF secretion and of hypoxia-guided neovascularization (Figures 4 and 5). Moreover, the recombinant RCR vACE-CREB enhanced the sensitivity of HepG2 and FLC4 cells to DOX treatment (Figure 3, Supplementary Figures 1 and 2). This increased sensitivity to DOX may result from the increase in activated caspase-3 (Figure 3), possibly due to the reduction in Bcl-2 and CCN1/CYR61 that are known to be activated by CREB.¹⁷

Logg *et al.*³³ injected MuLV-based RCR into a SC tumor in mice and 49 days later could not find MuLV (ZAPd-GFP) by PCR in a variety of organs (spleen, lung, kidney, liver or heart).³³ To fully validate these results, we are currently testing the spread of the recombinant viruses used in this study in our mouse model following injection adjacent to pre-formed xenografts, IV, IP both in the tumor and to other organs.

Total CREB and phosphorylated CREB proteins are both significantly elevated in HCC vs normal liver.^{2,20,21} We have shown previously that CREB has a pivotal role in HCC tumor progression by supporting angiogenesis and rendering HCC cells resistant to apoptosis.² These findings are in agreement with the results presented in this work. We demonstrate that the knockdown of CREB affected the viability of both HCC cell lines in hypoxia. Despite the less efficient reduction in the CREB mRNA and protein levels relative to HIF-1 or HIF-2 in HepG2 cells (Figure 2), it had a more prominent effect on survival (Figure 3). The 60% reduction in CREB protein increased dramatically the activation of caspase-3 and diminished cell viability under hypoxic conditions *in vitro* (Figure 3). Even knockdown of about 45% of CREB protein in HepG2 cells by vACE-X3 resulted in a reduction in cell viability and in an increase in activated caspase-3 after 72 h of hypoxia (Figure 3). Moreover, the growth of HepG2 cells expressing shRNA targeting CREB implanted in SCID mice reduced tumor growth (Figures 4 and 6).

The role of HIF-1 in response of tumor cells to hypoxia cue is well documented.⁴ Surprisingly, the significant knockdown of HIF-1 and HIF-2 did moderately (HIF-1) if at all (HIF-2) increase the sensitivity of HepG2 cells to the hypoxia cue *in vitro*. FLC4 cells had a similar sensitivity to CREB and HIF-1 knockdown in hypoxic conditions (Figure 3). However, FLC4 cells were more sensitive than HepG2 to DOX in normoxia and combining HIF-1 knockdown via vACE-HIF-1 and DOX in hypoxia resulted in a lower survival (Figure 3). Unlike the *in vitro* results, the growth of HepG2 tumors in mice was sensitive to the knockdown of either HIF-1 or HIF-2 (Figure 4). Tumors in which HIF-1 was knocked down had a reduced growth rate similar to tumors with reduced CREB, whereas tumors infected with vACE-HIF-2

had a more moderate but still significant attenuation of tumor growth.

HCC is one of the most vascular solid tumors, in which angiogenesis has an important role. Thus, knocking down the VEGF activator genes may affect the survival of HCC tumors (for a detailed review, see Yang and Poon⁴²). In agreement, the growth of HepG2 and VEGF expression was diminished in tumors expressing shRNA targeting HIF-1 or CREB (Figure 4).

Hypoxic areas express VEGF to attract blood vessels. When correlating the amount of hypoxia to the amount of blood vessel endothelial cells, there was a positive correlation in the vACE-NT-infected tumors, as expected. However, the knockdown of CREB, HIF-1 or both (vACE-X3) diminished the hypoxia-guided neovascularization significantly (Figure 4). We speculate that the misguided vessels have a major role in the diminished tumor growth of these tumors.

Throughout our work the efficient knockdown of HIF-2 had the smallest effect in response to hypoxia cue *in vitro* (Figure 3). However, knockdown of HIF-2 had some inhibition of tumor growth *in vivo* (Figure 4) although no significant effect on VEGF- or hypoxia-guided neovascularization was detected (Figure 5). The *in vitro* response of FLC4 and the *in vivo* response of HepG2 indicates that HIF-2 affects the response to hypoxia of HCC, albeit it is presented differently under different conditions in different cells. These results are in agreement with the results of He *et al.*⁵² that revealed that knockdown of HIF-2 or treatment with DOX had only a minor effect on HepG2 proliferation or VEGF expression.

The fact that cells harboring a MuLV provirus cannot be superinfected by MuLV led to the need to generate an RCR vector expressing a polycistronic shRNA sequence.³⁶ Moreover, targeting three different genes, each involved in the responses of the cells to hypoxia cue, should reduce the selection for siRNA-resistant cells. In this study we demonstrate that the expression of the three shRNA from the polycistronic RNA (vACE-X3) knocked down the three target genes, increased hypoxia-induced cell death and reduced secretion of VEGF *in vitro* and *in vivo* (Figures 2, 3 and 4). This finding suggested that the vACE-X3 may be effective in diminishing the survival of tumors cells in the hypoxic regions *in vivo*. However, although the growth of the HepG2 infected with vACE-X3 was diminished in mice relative to cells infected with vACE-NT, it was not as effective as infection of the cells with vACE-CREB or vACE-HIF-1 individually (Figure 4). This finding lead us to two avenues for further development of the system: (1) use either one of the RCR vectors vACE-CREB or vACE-HIF-1, or construct a RCR vector expressing a polycistronic shRNAs targeting only CREB and HIF-1; and (2) combining the RCRs with chemotherapy such as DOX.

It was suggested that CREB has multiple roles in drug resistance by activation of the human *mdr1* gene in HepG2 cells,⁵³ and protects tumor cells from dying by activation of the anti-apoptotic gene *bcl-2*.¹⁷ Moreover, phosphorylated CREB is required for DOX-induced tumor cell death.^{19,37} Here we showed that HepG2 tumor cells infected with vACE-CREB or vACE-X3 in mice were more sensitive to DOX treatment resulting in a reduction in tumor growth (Figure 6). The results presented in this work further emphasize the importance of the hypoxia-response regulators in survival of HCC, and the pivotal role of the CREB pathway in the resistance to DOX treatment. In addition, these results highlight the potential of MuLV-based recombinant RCRs in the treatment of solid tumors, both alone and in combination with chemotherapy. These results can lead to an improved efficacy and safety profile of the treatment that could result in fewer side effects, of which cardiomyopathy is a severe problem with DOX treatment.

CONFLICT OF INTEREST

The authors declare no conflict of interest.

ACKNOWLEDGEMENTS

This work was supported by a grant from the Israel Science Foundation and a grant from the Joint Research Fund between the Hebrew University Faculty of Medicine, and between Hadassah University Hospital (to Frenkel S) and by the Israel Cancer Association (to Honigman A).

REFERENCES

- 1 Dhanasekaran R, Limaye A, Cabrera R. Hepatocellular carcinoma: current trends in worldwide epidemiology, risk factors, diagnosis, and therapeutics. *Hepat Med* 2012; **4**: 19–37.
- 2 Abramovitch R, Tavor E, Jacob-Hirsch J, Zeira E, Amariglio N, Pappo O et al. A pivotal role of cyclic AMP-responsive element binding protein in tumor progression. *Cancer Res* 2004; **64**: 1338–1346.
- 3 Lu X, Kang Y. Hypoxia and hypoxia-inducible factors: master regulators of metastasis. *Clin Cancer Res* 2010; **16**: 5928–5935.
- 4 Rhim T, Lee DY, Lee M. Hypoxia as a target for tissue specific gene therapy. *J Control Release* 2013; **172**: 484–494.
- 5 Durand RE, Sham E. The lifetime of hypoxic human tumor cells. *Int J Radiat Oncol Biol Phys* 1998; **42**: 711–715.
- 6 Wu XZ, Xie GR, Chen D. Hypoxia and hepatocellular carcinoma: the therapeutic target for hepatocellular carcinoma. *J Gastroenterol Hepatol* 2007; **22**: 1178–1182.
- 7 Harris AL. Hypoxia—a key regulatory factor in tumour growth. *Nat Rev Cancer* 2002; **2**: 38–47.
- 8 Le QT, Denko NC, Giaccia AJ. Hypoxic gene expression and metastasis. *Cancer Metastasis Rev* 2004; **23**: 293–310.
- 9 Majmundar AJ, Wong WJ, Simon MC. Hypoxia-inducible factors and the response to hypoxic stress. *Mol Cell* 2010; **40**: 294–309.
- 10 Choi SH, Shin HW, Park JY, Yoo JY, Kim do Y, Ro WS et al. Effects of the knockdown of hypoxia inducible factor-1 alpha expression by adenovirus-mediated shRNA on angiogenesis and tumor growth in hepatocellular carcinoma cell lines. *Korean J Hepatol* 2010; **16**: 280–287.
- 11 Wenger RH. Cellular adaptation to hypoxia: O₂-sensing protein hydroxylases, hypoxia-inducible transcription factors, and O₂-regulated gene expression. *FASEB J* 2002; **16**: 1151–1162.
- 12 Holmquist-Mengelbier L, Fredlund E, Lofstedt T, Noguera R, Navarro S, Nilsson H et al. Recruitment of HIF-1alpha and HIF-2alpha to common target genes is differentially regulated in neuroblastoma: HIF-2alpha promotes an aggressive phenotype. *Cancer Cell* 2006; **10**: 413–423.
- 13 Hu CJ, Wang LY, Chodosh LA, Keith B, Simon MC. Differential roles of hypoxia-inducible factor 1alpha (HIF-1alpha) and HIF-2alpha in hypoxic gene regulation. *Mol Cell Biol* 2003; **23**: 9361–9374.
- 14 White PC, Shore AM, Clement M, McLaren J, Soeiro I, Lam EW et al. Regulation of cyclin D2 and the cyclin D2 promoter by protein kinase A and CREB in lymphocytes. *Oncogene* 2006; **25**: 2170–2180.
- 15 Mayr B, Montminy M. Transcriptional regulation by the phosphorylation-dependent factor CREB. *Nat Rev Mol Cell Biol* 2001; **2**: 599–609.
- 16 Aggarwal S, Kim SW, Ryu SH, Chung WC, Koo JS. Growth suppression of lung cancer cells by targeting cyclic AMP response element-binding protein. *Cancer Res* 2008; **68**: 981–988.
- 17 Belkhir A, Dar AA, Zaika A, Kelley M, El-Rifai W. t-Darpp promotes cancer cell survival by up-regulation of Bcl2 through Akt-dependent mechanism. *Cancer Res* 2008; **68**: 395–403.
- 18 Signorelli S, Jennings P, Leonard MO, Pfaller W. Differential effects of hypoxic stress in alveolar epithelial cells and microvascular endothelial cells. *Cell Physiol Biochem* 2010; **25**: 135–144.
- 19 Park SJ, Park SJ, Lee J, Kim HE, Sohn JW, Park YG. Inhibition of cyclic AMP response element-directed transcription by decoy oligonucleotides enhances tumor-specific radiosensitivity. *Biochem Biophys Res Commun* 2016; **469**: 363–369.
- 20 Kovach SJ, Price JA, Shaw CM, Theodorakis NG, McKillop IH. Role of cyclic-AMP responsive element binding (CREB) proteins in cell proliferation in a rat model of hepatocellular carcinoma. *J Cell Physiol* 2006; **206**: 411–419.
- 21 Yu L, Guo X, Zhang P, Qi R, Li Z, Zhang S. Cyclic adenosine monophosphate-responsive element-binding protein activation predicts an unfavorable prognosis in patients with hepatocellular carcinoma. *OncoTargets Ther* 2014; **7**: 873–879.
- 22 Block A, Freund CT, Chen SH, Nguyen KP, Finegold M, Windler E et al. Gene therapy of metastatic colon carcinoma: regression of multiple hepatic metastases by adenoviral expression of bacterial cytosine deaminase. *Cancer Gene Ther* 2000; **7**: 438–445.
- 23 Chen SH, Chen XH, Wang Y, Kosai K, Finegold MJ, Rich SS et al. Combination gene therapy for liver metastasis of colon carcinoma in vivo. *Proc Natl Acad Sci USA* 1995; **92**: 2577–2581.

- 24 Nyati MK, Symon Z, Kievit E, Dornfeld KJ, Rynkiewicz SD, Ross BD et al. The potential of 5-fluorocytosine/cytosine deaminase enzyme prodrug gene therapy in an intrahepatic colon cancer model. *Gene Ther* 2002; **9**: 844–849.
- 25 Zhang M, Li S, Nyati MK, DeRemer S, Parsels J, Rehemtulla A et al. Regional delivery and selective expression of a high-activity yeast cytosine deaminase in an intrahepatic colon cancer model. *Cancer Res* 2003; **63**: 658–663.
- 26 Sung MW, Yeh HC, Thung SN, Schwartz ME, Mandeli JP, Chen SH et al. Intratumoral adenovirus-mediated suicide gene transfer for hepatic metastases from colorectal adenocarcinoma: results of a phase I clinical trial. *Mol Ther* 2001; **4**: 182–191.
- 27 Logg CR, Robbins JM, Jolly DJ, Gruber HE, Kasahara N. Retroviral replicating vectors in cancer. *Methods Enzymol* 2012; **507**: 199–228.
- 28 Roe T, Reynolds TC, Yu G, Brown PO. Integration of murine leukemia virus DNA depends on mitosis. *EMBO J* 1993; **12**: 2099–2108.
- 29 Miller DG, Adam MA, Miller AD. Gene transfer by retrovirus vectors occurs only in cells that are actively replicating at the time of infection. *Mol Cell Biol* 1990; **10**: 4239–4242.
- 30 Hiraoka K, Kimura T, Logg CR, Tai CK, Haga K, Lawson GW et al. Therapeutic efficacy of replication-competent retrovirus vector-mediated suicide gene therapy in a multifocal colorectal cancer metastasis model. *Cancer Res* 2007; **67**: 5345–5353.
- 31 Tai CK, Kasahara N. Replication-competent retrovirus vectors for cancer gene therapy. *Front Biosci* 2008; **13**: 3083–3095.
- 32 Logg CR, Logg A, Matusik RJ, Bochner BH, Kasahara N. Tissue-specific transcriptional targeting of a replication-competent retroviral vector. *J Virol* 2002; **76**: 12783–12791.
- 33 Logg CR, Tai CK, Logg A, Anderson WF, Kasahara N. A uniquely stable replication-competent retrovirus vector achieves efficient gene delivery in vitro and in solid tumors. *Hum Gene Ther* 2001; **12**: 921–932.
- 34 Sliva K, Schnierle BS. Selective gene silencing by viral delivery of short hairpin RNA. *Viral J* 2010; **7**: 248.
- 35 McIntyre GJ, Arndt AJ, Gillespie KM, Mak WM, Fanning GC. A comparison of multiple shRNA expression methods for combinatorial RNAi. *Genet Vaccines Ther* 2011; **9**: 9.
- 36 Sliva K, Schnierle BS. Stable integration of a functional shRNA expression cassette into the murine leukemia virus genome. *Virology* 2006; **351**: 218–225.
- 37 Li T, Liu Z, Jiang K, Ruan Q. Angiopoietin2 enhances doxorubicin resistance in HepG2 cells by upregulating survivin and Ref-1 via MSK1 activation. *Cancer Lett* 2013; **337**: 276–284.
- 38 Sayan M, Shukla A, MacPherson MB, Macura SL, Hillegass JM, Perkins TN et al. Extracellular signal-regulated kinase 5 and cyclic AMP response element binding protein are novel pathways inhibited by vandetanib (ZD6474) and doxorubicin in mesotheliomas. *Am J Respir Cell Mol Biol* 2014; **51**: 595–603.
- 39 Tanaka T, Yamaguchi J, Shoji K, Nangaku M. Anthracycline inhibits recruitment of hypoxia-inducible transcription factors and suppresses tumor cell migration and cardiac angiogenic response in the host. *J Biol Chem* 2012; **287**: 34866–34882.
- 40 Gilliam LA, Moylan JS, Ann Callahan L, Sumanda MP, Reid MB. Doxorubicin causes diaphragm weakness in murine models of cancer chemotherapy. *Muscle Nerve* 2011; **43**: 94–102.
- 41 Meyuhas R, Pikarsky E, Tavor E, Klar A, Abramovitch R, Hochman J et al. A key role for cyclic AMP-responsive element binding protein in hypoxia-mediated activation of the angiogenesis factor CCN1 (CYR61) in tumor cells. *Mol Cancer Res* 2008; **6**: 1397–1409.
- 42 Yang ZF, Poon RT. Vascular changes in hepatocellular carcinoma. *Anat Rec* 2008; **291**: 721–734.
- 43 Ryan HE, Lo J, Johnson RS. HIF-1 alpha is required for solid tumor formation and embryonic vascularization. *EMBO J* 1998; **17**: 3005–3015.
- 44 Jeon SH, Chae BC, Kim HA, Seo GY, Seo DW, Chun GT et al. The PKA/CREB pathway is closely involved in VEGF expression in mouse macrophages. *Mol Cells* 2007; **23**: 23–29.
- 45 Zhu AX, Duda DG, Sahani DV, Jain RK. HCC and angiogenesis: possible targets and future directions. *Nat Rev Clin Oncol* 2011; **8**: 292–301.
- 46 Kizaka-Kondoh S, Inoue M, Harada H, Hiraoka M. Tumor hypoxia: a target for selective cancer therapy. *Cancer Sci* 2003; **94**: 1021–1028.
- 47 Tai CK, Wang W, Lai YH, Logg CR, Parker WB, Li YF et al. Enhanced efficiency of prodrug activation therapy by tumor-selective replicating retrovirus vectors armed with the *Escherichia coli* purine nucleoside phosphorylase gene. *Cancer Gene Ther* 2010; **17**: 614–623.
- 48 Tai CK, Wang WJ, Chen TC, Kasahara N. Single-shot, multicycle suicide gene therapy by replication-competent retrovirus vectors achieves long-term survival benefit in experimental glioma. *Mol Ther* 2005; **12**: 842–851.
- 49 Wang WJ, Tai CK, Kasahara N, Chen TC. Highly efficient and tumor-restricted gene transfer to malignant gliomas by replication-competent retroviral vectors. *Hum Gene Ther* 2003; **14**: 117–127.

- 50 Takahashi M, Valdes G, Hiraoka K, Inagaki A, Kamijima S, Micewicz E *et al*. Radiosensitization of gliomas by intracellular generation of 5-fluorouracil potentiates prodrug activator gene therapy with a retroviral replicating vector. *Cancer Gene Ther* 2014; **21**: 405–410.
- 51 Huang TT, Hlavaty J, Ostertag D, Espinoza FL, Martin B, Petznek H *et al*. Toca 511 gene transfer and 5-fluorocytosine in combination with temozolomide demonstrates synergistic therapeutic efficacy in a temozolomide-sensitive glioblastoma model. *Cancer Gene Ther* 2013; **20**: 544–551.
- 52 He C, Sun XP, Qiao H, Jiang X, Wang D, Jin X *et al*. Downregulating hypoxia-inducible factor-2alpha improves the efficacy of doxorubicin in the treatment of hepatocellular carcinoma. *Cancer Sci* 2012; **103**: 528–534.
- 53 Ye CG, Yeung JH, Huang GL, Cui P, Wang J, Zou Y *et al*. Increased glutathione and mitogen-activated protein kinase phosphorylation are involved in the induction

of doxorubicin resistance in hepatocellular carcinoma cells. *Hepatol Res* 2013; **43**: 289–299.



This work is licensed under a Creative Commons Attribution-NonCommercial-NoDerivs 4.0 International License. The images or other third party material in this article are included in the article's Creative Commons license, unless indicated otherwise in the credit line; if the material is not included under the Creative Commons license, users will need to obtain permission from the license holder to reproduce the material. To view a copy of this license, visit <http://creativecommons.org/licenses/by-nc-nd/4.0/>

© The Author(s) 2017

Supplementary Information accompanies the paper on *Cancer Gene Therapy* website (<http://www.nature.com/cgt>)